

GW231109_235456: A Sub-threshold Binary Neutron Star Merger in the LIGO–Virgo–KAGRA O4a Observing Run?

WANTING NIU ^{1,2} CHAD HANNA^{1,2,3,4} CARL-JOHAN HASTER ^{5,6} SHOMIK ADHICARY ^{1,2} PRATYUSAVA BARAL ⁷,
AMANDA BAYLOR ⁷ BRYCE COUSINS ^{8,1,2} JOLIEN D. E. CREIGHTON ⁷ HEATHER FONG^{9,10,11}
YUN-JING HUANG ^{1,2} RACHAEL HUXFORD¹² PRATHAMESH JOSHI ^{1,2,13} JAMES KENNINGTON ^{1,2}
ALVIN K. Y. LI ^{10,11} RYAN MAGEE ¹⁴ DUNCAN MEACHER ⁷ CODY MESSICK ⁷ SOICHIRO MORISAKI ¹⁵
CORT POSNANSKY ^{1,2} SURABHI SACHDEV ¹³ SHIO SAKON ^{1,2} URJA SHAH ¹³ DIVYA SINGH ¹⁶ RON TAPIA^{1,4}
LEO TSUKADA ^{5,6} AARON VIETS ¹⁷ ZACH YARBROUGH ¹⁸ AND NOAH ZHANG ¹³

¹*Department of Physics, The Pennsylvania State University, University Park, PA 16802, USA*

²*Institute for Gravitation and the Cosmos, The Pennsylvania State University, University Park, PA 16802, USA*

³*Department of Astronomy and Astrophysics, The Pennsylvania State University, University Park, PA 16802, USA*

⁴*Institute for Computational and Data Sciences, The Pennsylvania State University, University Park, PA 16802, USA*

⁵*Department of Physics and Astronomy, University of Nevada, Las Vegas, 4505 South Maryland Parkway, Las Vegas, NV 89154, USA*

⁶*Nevada Center for Astrophysics, University of Nevada, Las Vegas, NV 89154, USA*

⁷*Leonard E. Parker Center for Gravitation, Cosmology, and Astrophysics, University of Wisconsin-Milwaukee, Milwaukee, WI 53201, USA*

⁸*Department of Physics, University of Illinois, Urbana, IL 61801 USA*

⁹*Department of Physics and Astronomy, University of British Columbia, Vancouver, BC, V6T 1Z4, Canada*

¹⁰*RESCEU, The University of Tokyo, Tokyo, 113-0033, Japan*

¹¹*Graduate School of Science, The University of Tokyo, Tokyo 113-0033, Japan*

¹²*Minnesota Supercomputing Institute, University of Minnesota, Minneapolis, MN 55455, USA*

¹³*School of Physics, Georgia Institute of Technology, Atlanta, GA 30332, USA*

¹⁴*LIGO Laboratory, California Institute of Technology, Pasadena, CA 91125, USA*

¹⁵*Institute for Cosmic Ray Research, The University of Tokyo, 5-1-5 Kashiwanoha, Kashiwa, Chiba 277-8582, Japan*

¹⁶*Department of Physics, University of California, Berkeley, CA 94720, USA*

¹⁷*Concordia University Wisconsin, Mequon, WI 53097, USA*

¹⁸*Department of Physics and Astronomy, Louisiana State University, Baton Rouge, LA 70803, USA*

ABSTRACT

We present a sub-threshold search for gravitational-wave inspirals from binary neutron stars using data from the first part of the fourth observing run of the LIGO–Virgo–KAGRA Collaboration. To enhance sensitivity to this targeted population, we incorporate a redshift-corrected population model—based on radio observations of Galactic double neutron star systems. The search identifies a significant trigger with a false-alarm rate of 1 per 50 years and a network signal-to-noise ratio of 9.7, which was first reported by the LVK in low-latency processing as S231109ci and subsequently in the GWTC-4.0 catalog as GW231109_235456, a sub-threshold candidate. Accounting for a trials factor of five from the four LVK searches in GWTC-4.0 and this new search, the false-alarm rate of the reported candidate is approximately 1 per 10 years. If this event is of astrophysical origin, the inferred source properties indicate component masses of $1.40 - 2.24 M_{\odot}$ for the primary and $0.97 - 1.49 M_{\odot}$ for the secondary, yielding a total mass of $2.95^{+0.38}_{-0.07} M_{\odot}$; the event was localized to a region of 450 deg^2 (90% probability) at a luminosity distance of $165^{+70}_{-69} \text{ Mpc}$.

Keywords: Gravitational Waves — Neutron Stars — Compact Binary Merger — Data Analysis

1. INTRODUCTION

The first binary neutron star (BNS) merger, GW170817, was discovered by the Laser Interferometer Gravitational-Wave Observatory (LIGO) (Aasi et al.

2015) and Virgo (Acernese et al. 2015) more than eight years ago. GW170817 was simultaneously observed with GRB170817A and subsequently observed across the electromagnetic spectrum (Abbott et al. 2017a,b). A second gravitational-wave (GW) BNS candidate, GW190425 (Abbott et al. 2020), was detected more than six years ago and no electromagnetic counterparts were detected. The fourth operation of LIGO Scientific, Virgo and KAGRA Collaboration (LVK) (Abbott et al. 2016; Aasi et al. 2015; Acernese et al. 2015) has been observing since May 2023 with unprecedented GW sensitivity (Soni et al. 2025; Capote et al. 2025; Buikema et al. 2020; Ganapathy et al. 2023; Jia et al. 2024; Tse et al. 2019). Nevertheless, few significant BNS candidates have been identified, either in real-time searches or in the latest Gravitational Wave Transient Catalog (GWTC) reporting candidates from the first part of the fourth observing run (O4a). As GWTC-4.0 (Abac et al. 2025a) reported no significant BNS candidates, the question naturally emerges: “Where are the electromagnetically bright binary neutron stars?”

It is plausible that at least one hidden BNS signal with signal-to-noise ratio (SNR) ~ 10 in the LVK O4a data went undetected, as previous searches considered a large parameter space including neutron star–black hole binary (NSBH) and binary black hole (BBH) sources beyond BNS. Due to the template bank size in such broad searches, sensitivity is maintained across all stellar populations but is not specifically optimized for BNS signals, particularly for our hypothesis concerning a specific BNS population. In this work, we target BNS systems guided by the Galactic double neutron star (DNS) catalog as a representative BNS population that is considerably narrower than the GW populations searched for previously in O4a (Abac et al. 2025a) to explore sub-threshold BNS candidates. We note that the properties of GW170817 are consistent with the Galactic DNS catalog. This population, including GW170817, has been measured with identified electromagnetic counterparts. A similar sub-threshold search was carried out in the first observing run (O1) (Magee et al. 2019), yielding a null result.

For our purposes, DNS systems constitute a narrow mass population of binaries with two neutron stars found by radio telescopes (Özel & Freire 2016; Thorsett & Chakrabarty 1999), including the first discovered BNS (Hulse & Taylor 1975). Previous studies have shown strong consistency between the component masses of GW170817 and this population (Abbott et al. 2017a, 2019; Zhang et al. 2019; Galaudage et al. 2021). By contrast, GW190425 (Abbott et al. 2020) had components each consistent with isolated neutron star masses but

outside the DNS distribution, leading to interpretations that it came from a fast-merging population of massive two neutron star systems (Romero-Shaw et al. 2020a; Safarzadeh et al. 2020) or possibly contained one or more black hole (BH) components (Clesse & Garcia-Bellido 2022; Gupta et al. 2020; Foley et al. 2020; Kyutoku et al. 2020; Singh et al. 2021). Moreover, no electromagnetic counterpart was observed for GW190425 (Abbott et al. 2020; Foley et al. 2020; Coulter et al. 2025; Paek et al. 2024).

As a result, BNS systems similar to GW190425 are less relevant for the target population in this study. Depending on the SNR of potential GW190425-like events, our search could naturally down-rank their significance. In contrast, there is particular interest in identifying and improving the detection rate of GW170817-like systems, since they are known to produce electromagnetic counterparts (Abbott et al. 2017a, 2019; Valenti et al. 2017; McCully et al. 2017; Smartt et al. 2017; Evans et al. 2017; Kilpatrick et al. 2017) and may synthesize a significant amount of r-process elements (Drout et al. 2017; Pian et al. 2017). These results offer a clearer view of the contribution of BNS mergers to r-process element abundances in galaxies. For simplicity, we designate our target population as DNS throughout this paper.

We organize the paper as follows. In Sec 2, we describe our search design, including the choice of population model and parameter space. In Sec 3, we present the most significant candidate in our analysis and its source properties. In Sec 4, we examine this candidate in more detail and explore its physical implications. The DNS catalog is provided in the Appendix.

2. SEARCH DESCRIPTION

We search for GW inspirals from DNS mergers using the GstLAL matched-filtering pipeline (Cannon et al. 2012; Messick et al. 2017; Sachdev et al. 2019; Hanna et al. 2020; Cannon et al. 2020; Sakon et al. 2024; Ray et al. 2023; Tsukada et al. 2023; Ewing et al. 2024; Joshi et al. 2025a,b), which correlates detector data with banks of waveform templates (Owen 1996; Hanna et al. 2023). The GstLAL pipeline was used for the results in GWTC-4.0 (Abac et al. 2025a), and we use its latest improvements (Joshi et al. 2025b,a). Our sub-threshold search differs from the standard search in GWTC-4.0 by applying a mass model of DNS population (Sec 2.1) to enhance sensitivity to our targets and by using a denser template bank in the DNS mass range (Sec 2.2) to reduce signal loss (Owen 1996). Candidate triggers are ranked by the GstLAL likelihood-ratio function (Cannon et al. 2013; Tsukada et al. 2023), which includes the mass model as a prior (Fong 2018; Ray et al. 2023).

GWTC-4.0 used a power-law prior in mass and covered a much broader component mass and spin space (Abac et al. 2025b). The ratio of prior volumes between this work and GWTC-4.0 is roughly 5×10^{-7} , motivating the potential to dig out a BNS system (see Appendix B). Further details on the astrophysical population model employed in the DNS mass model for this search are provided in Sec. 2.1.

2.1. Population Model

As the catalog of DNS systems observed in radio surveys grows, several models have been proposed to describe their mass distribution. Early studies suggested a narrow Gaussian (Thorsett & Chakrabarty 1999; Özel et al. 2012), later extended to a broader Gaussian with the discovery of heavier systems (Kiziltan et al. 2013; Özel & Freire 2016). After GW170817, Farrow et al. (2019) supported a two-component Gaussian model for the recycled neutron star in the binary. Although studies of GW binaries containing at least one neutron star suggest a broader mass distribution with an excess of high-mass components (Abbott et al. 2023; Landry & Read 2021), our focus here is on DNS population that remain consistent with radio observations. The limited number of observed DNS systems prevents a definitive conclusion. Given these conditions, we determine the mass function in our ranking statistic by collecting the latest DNS catalog and fitting it to the proposed distributions. Table 3 lists the mass measurements of these DNS systems, including the multi-messenger event GW170817. As of May 2025, 19 DNS systems have been discovered in radio surveys, with 13 offering precise individual mass measurements. From these well-measured systems, 26 neutron star masses are obtained, which are well described by a two-component Gaussian distribution,

$$f(x) = w \cdot \frac{1}{\sqrt{2\pi\sigma_1^2}} \exp\left(-\frac{(x - \mu_1)^2}{2\sigma_1^2}\right) + (1 - w) \cdot \frac{1}{\sqrt{2\pi\sigma_2^2}} \exp\left(-\frac{(x - \mu_2)^2}{2\sigma_2^2}\right), \quad (1)$$

where w is the mixing weight for the first Gaussian component, μ_1 and μ_2 are the peaks of the two Gaussian components, and σ_1 and σ_2 are the widths of the two Gaussian components. These parameter values are determined by a fit as shown in Fig. 1. Our fitted model resembles that of Alsing et al. (2018), although their study includes neutron star–white dwarf systems beyond DNS, whose mergers lie outside the frequency range of LVK detectors (Nelemans 2003).

The DNS catalog reports neutron star masses in the source frame, while the search pipeline observes events

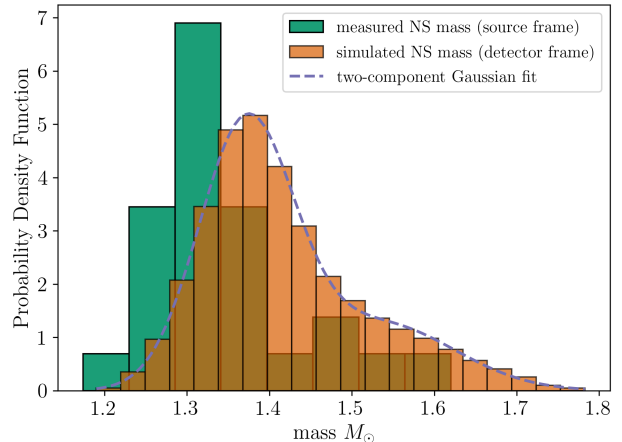


Figure 1. Mass distribution for the DNS population model adopted in this study. The green color represents the mass distribution from direct measurements of 13 DNS systems. The orange color represents the simulated results obtained by sampling the source-frame distribution in a comoving frame. The purple dashed line shows the fitted mass distribution in the detector frame, which is incorporated into the mass-model function used for this search.

in the detector frame, requiring a redshift correction. This effect is small, as detected DNS systems, notably GW170817, have redshifts below ~ 0.1 (Abbott et al. 2017a). We account for cosmological redshift in our population model by sampling simulated DNS events in the comoving frame. Component masses in the source frame are drawn from a joint two-component Gaussian distribution in (m_1, m_2) , with $m_2 \leq m_1$ and $m_2/m_1 > 0.5$. Redshifts are sampled from the distribution $p(z) \propto \mathcal{R}(z) \frac{dV_c}{dz} \frac{1}{1+z}$ (Essick et al. 2025; Ye & Fishbach 2021; Abbott et al. 2023; gwt 2025) assuming a constant source-frame merger rate and uniformity in comoving volume. The comoving volume element dV_c/dz is evaluated under the standard cosmology (Ade et al. 2016), following Ye & Fishbach (2021); Essick et al. (2025). We impose a sensitivity cutoff based on the measured LIGO O4a performance (Abac et al. 2025c), requiring a minimum network SNR of 8.0, yielding the projected high-SNR DNS population in the detector frame. We perform the sampling using the `monte-carlo-vt` (Essick & et al. 2025) and `gw-distributions` (Essick 2025) software packages. Assuming that the redshift-corrected distribution remains well described by a two-component Gaussian, we re-fit the sampled distribution, obtaining the following parameter values: $w = 0.7137$, $\mu_1 = 1.372$, $\mu_2 = 1.534$, $\sigma_1 = 0.05768$, and $\sigma_2 = 0.09102$. Fig. 1 shows the measured neutron star masses in the source frame, the simulated neutron star masses in the detector frame, and the corresponding two-component Gaussian

Parameter	DNS Search
Primary Mass, m_1^{det}	$\in [1.1, 2.1] M_\odot$
Secondary Mass, m_2^{det}	$\in [1.1, 2.1] M_\odot$
Mass Ratio, $q = m_2^{\text{det}}/m_1^{\text{det}}$	$\in [0.7, 1.0]$
Chirp Mass, \mathcal{M}^{det}	$\in [0.957, 1.82] M_\odot$
Total Mass, M_T^{det}	$\in [2.3, 3.6] M_\odot$
Dimensionless Component Spin, $s_{i,z}$	$\in [-0.05, 0.05]$
Effective Spin, χ_{eff}	$\in [-0.05, 0.05]$
Lower Frequency cut-off	15 Hz
Higher Frequency cut-off	1024 Hz
Waveform approximant	IMRPhenomD
Minimum match	99 %
Total number of templates	360600

Table 1. Parameter space of the DNS template bank. Based on the DNS distribution in the detector frame, templates are placed for component masses in $[1.1, 2.1] M_\odot$ with a mass ratio $q = m_2^{\text{det}}/m_1^{\text{det}} \in [0.7, 1.0]$, and spins are set according to the assumed low-spin parameter of BNS mergers.

fit. In the full mass-model term of the ranking statistic, the population model is further weighted by template migration and volume factors (Ray et al. 2023; Fong 2018).

2.2. Search Parameter Space

We design a DNS-targeted bank with improved sensitivity by restricting the template mass range to the detector-frame DNS population, increasing the template duration, and raising the minimum match (Owen 1996) used in bank placement. The bank is generated using manifold (Hanna 2024; Hanna et al. 2023). Table 1 summarizes the parameter space of this bank.

When sampling detector-frame simulated events in 2.1, we adopt a source-frame mass range extending 3σ below the first peak and 2σ above the second. This corresponds to a detector-frame range of $[1.190, 1.753] M_\odot$. To mitigate edge effects at the template-bank boundaries and ensure robust recovery across the population, we extend the bank bounds to $[1.1, 2.1] M_\odot$. This component mass range corresponds to a chirp mass $\mathcal{M} = (m_1 m_2)^{3/5} / (m_1 + m_2)^{1/5}$ range of $[0.957, 1.82] M_\odot$. Based on the distribution in Table 3, the bank is further restricted to semi-equal mass ratios and realistic DNS total masses. Fig 2 displays the mass parameter space of the template bank, along with the weighting values from the DNS mass model. The one-dimensional population model described in 2.1 is extended to a two-dimensional probability factor $p(m_1, m_2) = p(m_1) * p(m_2)$. Both $p(m_1)$ and $p(m_2)$ are derived from the fitted function presented in 2.1.

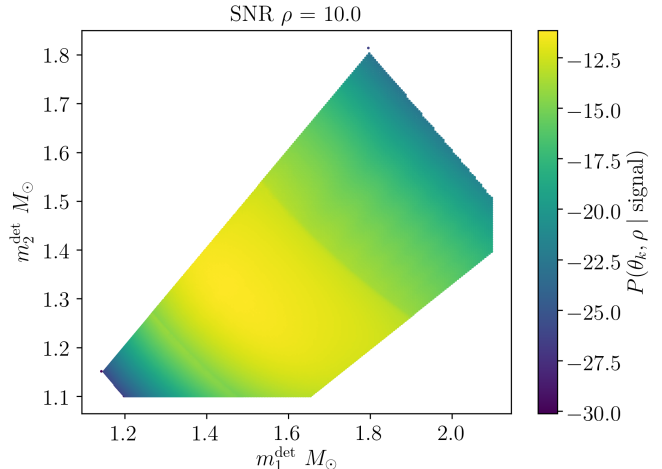


Figure 2. Template bank designed for the DNS-targeted search in the (m_1, m_2) parameter space of detector frame. The color bar indicates the mass-model weighting probability derived from the population model shown in Fig. 1.

Radio observations show most DNS systems possess low spins at the merger stage (Zhu et al. 2018). Accordingly, we restrict the dimensionless component spins to the range $[-0.05, 0.05]$ in the template bank, consistent with previous searches (Sakon et al. 2024; Abac et al. 2025b). We also assume the component spin to be aligned with the orbital angular momentum. Compared with previous searches (Sakon et al. 2024), we adopt a lower frequency cutoff of 15 Hz without imposing a maximum duration cutoff. The upper frequency cutoff of the waveform is set to 1024 Hz, and the waveform is modeled using IMRPhenomD (Khan et al. 2016a; Husa et al. 2016). Additionally, we increase the minimum match from 0.97 to 0.99 in bank placement, reducing the SNR loss due to parameter discretization from 3% to 1% (Owen 1996).

3. RESULT

We analyzed data collected from 24 May 2023 15:00:00 UTC to 16 January 2024 16:00:00 UTC, by the two interferometers (IFOs) at LIGO-Hanford (LHO) and LIGO-Livingston (LLO), spanning the observing run of LVK O4a. Details regarding data quality are available in Abac et al. (2025c,b). In this period, we identified a coincident event of high significance, with a false-alarm rate (FAR) of 1 per 50 years and a network SNR of 9.7. This candidate also appears in the low-latency event repository GraceDB (LVK 2018) as the sub-threshold super-event S231109ci, albeit with a much higher FAR, and is reported as GW231109_235456 in Abac et al. (2025a), the GstLAL O4a candidate with the highest probability of being a BNS. To further characterize the

Table 2. Properties of the GW candidate GW231109.235456 detected in the sub-threshold search during O4a, including the detection statistic, event time, recovered template parameters from the search pipeline, source parameters estimated under low-spin priors, and source parameters estimated under high-spin priors. For the source parameters, we report \mathcal{M}^{det} , \mathcal{M} , M , χ_{eff} and D_L as medians with symmetric 90% credible intervals (CIs); m_1 , Θ and Λ_S are reported as a 0 – 90 percentile CI; m_2 and q are reported as a 10 – 100 percentile CI; $\Delta\Omega$ is reported as a 90% credible region.

Detection Statistics	
false alarm rate (FAR) (yr^{-1})	0.02
FAR after GWTC-4.0 trials (yr^{-1})	0.1
Network SNR	9.7
Instruments	HL
Time	
GPS time (s)	1383609314.057
UTC time	9 Nov 2023, 23:54:56
Recovered Template Parameters	
Detector-frame chirp mass, \mathcal{M}^{det} (M_\odot)	1.306
Detector-frame primary mass, m_1^{det} (M_\odot)	1.78
Detector-frame secondary mass, m_2^{det} (M_\odot)	1.27
Inferred Parameter: Low-spin priors ($ \chi \leq 0.05$)	
Detector-frame chirp mass \mathcal{M}^{det} (M_\odot)	$1.3063^{+0.0003}_{-0.0003}$
Chirp mass \mathcal{M} (M_\odot)	$1.260^{+0.019}_{-0.018}$
Primary mass m_1 (M_\odot)	1.40 – 1.65
Secondary mass m_2 (M_\odot)	1.27 – 1.49
Mass ratio $q = m_2/m_1$	0.77 – 1.00
Total mass M (M_\odot)	$2.90^{+0.05}_{-0.04}$
Effective spin χ_{eff}	$0.014^{+0.016}_{-0.015}$
Luminosity distance D_L (Mpc)	169^{+72}_{-70}
Viewing angle Θ (deg)	0 – 60
Localization area $\Delta\Omega$ (deg^2)	460
Symmetric tidal deformability Λ_S	0 – 2700
Inferred Parameter: High-spin priors ($ \chi \leq 0.40$)	
Detector-frame chirp mass \mathcal{M}^{det} (M_\odot)	$1.3067^{+0.0006}_{-0.0005}$
Chirp mass \mathcal{M} (M_\odot)	$1.261^{+0.018}_{-0.018}$
Primary mass m_1 (M_\odot)	1.40 – 2.24
Secondary mass m_2 (M_\odot)	0.97 – 1.49
Mass ratio $q = m_2/m_1$	0.43 – 1.00
Total mass M (M_\odot)	$2.95^{+0.38}_{-0.07}$
Effective spin χ_{eff}	$0.051^{+0.103}_{-0.035}$
Luminosity distance D_L (Mpc)	165^{+70}_{-69}
Viewing angle Θ (deg)	0 – 60
Localization area $\Delta\Omega$ (deg^2)	450
Symmetric tidal deformability Λ_S	0 – 3000

source, we performed parameter estimation on this event using `bilby` (Ashton et al. 2019; Romero-Shaw et al. 2020b). The detection and parameter estimation information for this trigger is summarized in Table 2.

We perform a Bayesian analysis in the frequency range 20.0 – 972.8 Hz using 256.0 seconds of data containing the GW231109.235456 event, following Abac

et al. (2025b). The waveform is modeled with `IMRPhenomPv2_NRTidalv2` (Hannam et al. 2014; Khan et al. 2016b; Dietrich et al. 2019; Colleoni et al. 2025), matching the data to predicted waveforms beyond the search parameter space. We employ a reduced-order quadrature (ROQ) likelihood in `bilby` to minimize the computational cost of the Bayesian analysis (Smith et al. 2016; Morisaki et al. 2023). For the parameter estimation analysis, we estimate the noise spectrum for the specific duration and bandwidth of data under analysis using the `BayesWave` algorithm (Littenberg & Cornish 2015; Gupta & Cornish 2024). We also marginalize over the uncertainty in the calibration of the data (Abac et al. 2025b). Unless otherwise noted, all bounds on GW231109.235456 properties reported in the text and Table 2 correspond to 90% posterior probability credible intervals (CIs). No glitches or data-quality issues are observed near the event; therefore, no glitch subtraction is applied.

We consider two priors on the source properties: a low-spin prior with $|\chi| \leq 0.05$ and a high-spin prior with $|\chi| \leq 0.40$, both assuming isotropic spin distributions. The detector-frame chirp mass \mathcal{M}^{det} is restricted to 1.30 – 1.31, as informed by the search, and the detector-frame component masses m_1^{det} and m_2^{det} are limited to 0.3 – 5.0 with a mass ratio constraint of $m_2/m_1 \geq 1/8$; further discussion of these parameters in the context of BNS mergers can be found in the parameter-estimation results for GW170817 (Abbott et al. 2019). The masses presented in Table 2 have been converted from the detector-frame through a redshift inferred from the measured luminosity distance and a cosmology from Ade et al. (2016); Price-Whelan et al. (2022). As this is a BNS-targeted search, we also account for tidal deformation of the neutron stars (NSs) by adopting a uniform prior on the symmetric combination, $\Lambda_S = \frac{1}{2}(\Lambda_1 + \Lambda_2)$, in the range 0–5000 and assume a common equation-of-state-independent relation between the individual NS tidal deformabilities Λ_1 and Λ_2 (Yagi & Yunes 2016; Chatziioannou et al. 2018), which are in turn also constrained to the range 0–5000. The posterior of Λ_S spans the entire prior range, but excludes values above 3000 (2700) at a 90% credible level for the high-spin (low-spin) prior. Additionally, this constraint can be reformulated into a bound on the combined dimensionless tidal deformability (Abbott et al. 2017a),

$$\tilde{\Lambda} = \frac{16}{13} \frac{(m_1 + 12m_2)m_1^4\Lambda_1 + (m_2 + 12m_1)m_2^4\Lambda_2}{(m_1 + m_2)^5}. \quad (2)$$

By reweighting the inferred posterior distributions of $\tilde{\Lambda}$ to be consistent with a uniform prior over $\tilde{\Lambda}$ itself, we can place an one-sided upper bound of 4500 (3700) at a 90%

credible level for the high-spin (low-spin) prior. Higher-order parameters are less constrained in this result due to the absence of EM counterpart, since this event was identified in a high-latency analysis. Given the moderate SNR, the posteriors for the tidal parameters provide limited information on the NS equation of state (EoS) from this event alone. To verify this claim, two additional analysis variants were performed, one where we assume that both binary components are BHs (with $\Lambda_1 = \Lambda_2 = 0$) and one where the binary components can be tidally deformed but without restricting them to follow a common EoS (allowing Λ_1 and Λ_2 to vary independently in the range 0–5000) as assumed in the main analysis above. For the high-spin (low-spin) priors, we prefer the main analysis with a \log_{10} Bayes Factor of 0.09 (−0.23) relative to the BH assumption and a \log_{10} Bayes Factor of 0.12 (0.39) relative to the independent Λ assumption. We additionally prefer the high-spin analysis over the low-spin one with a \log_{10} Bayes Factor of 0.33. Hence, for the moderately favoured high-spin prior we infer a weak preference for the analysis where GW231109.235456 is described as a BNS following a common NS EoS over both of the other more general compact-object binary variants. The inferred masses, shown in Fig 3, are consistent with the DNS population and overlap with the inferred component masses of GW170817 (Abbott et al. 2019). We also note that for both prior choices, but more prominently so for the high-spin analysis, we infer a positive effective inspiral spin χ_{eff} . Table 2 summarizes the posterior constraints on source properties, sky localization, and viewing angle.

4. DISCUSSION

In this work, we present a targeted search for GWs from BNS sources in O4a, motivated by the catalog of Galactic DNS systems. We identify a single candidate of interest, previously reported by the LVK as the sub-threshold event GW231109.235456. Our analysis yields a FAR of 1 per 50 years, which, after applying a trials factor of five to account for the four GWTC-4.0 searches (Abac et al. 2025a) and the present work, corresponds to 1 per 10 years. While the low SNR precludes a definitive association with a BNS merger, the observation is fully consistent with known BNS merger rates. In particular, the accumulated hypervolume for BNS signals in O4a was $5.28 \times 10^{-3} \text{ Gpc}^3 \text{ yr}$ (Abac et al. 2025c), implying a rate of $\sim 200 \text{ Gpc}^{-3} \text{ yr}^{-1}$ from this single event, well within the current inferred range of 7.6–250 $\text{Gpc}^{-3} \text{ yr}^{-1}$ (gwt 2025). We encourage a systematic review of possible multimessenger counterparts to this sub-threshold candidate. A skymap of the event is

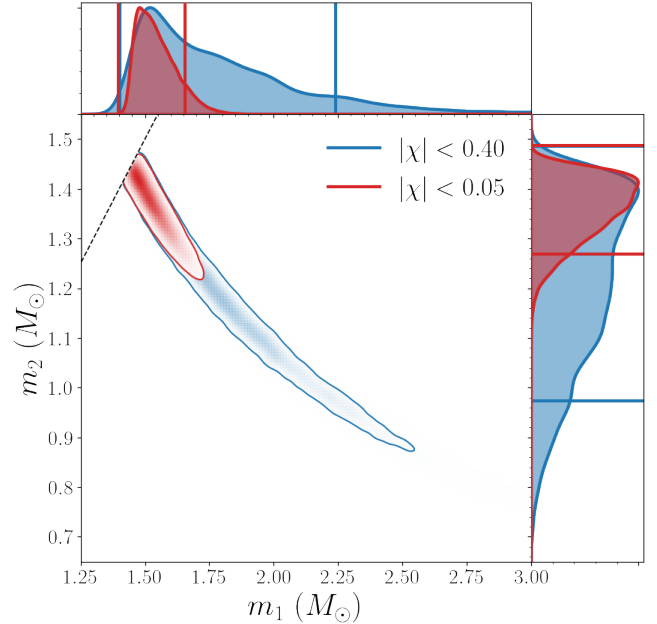


Figure 3. Posterior distributions for the binary component masses m_1 and m_2 for the high-spin ($|\chi| \leq 0.40$; blue) and low-spin ($|\chi| \leq 0.05$; red) analyses. A dashed line marks the equal-mass limit of $q = 1$ in the two-dimensional plot. The vertical lines in the one-dimensional plots enclose 90% of the posterior probability and correspond to the ranges given in Table 2. The one-dimensional distributions have been normalized to have equal maxima.

provided on the GraceDB page of superevent S231109ci and in the accompanying data release.

ACKNOWLEDGMENTS

This research has made use of data, software and/or web tools obtained from the Gravitational Wave Open Science Center (<https://www.gw-openscience.org/>), a service of LIGO Laboratory, the LIGO Scientific Collaboration (LSC) and the Virgo Collaboration. We especially made heavy use of the LVK Algorithm Library. LIGO was constructed by the California Institute of Technology and the Massachusetts Institute of Technology with funding from the United States National Science Foundation (NSF) and operates under cooperative agreements PHYS-0757058 and PHY-0823459. In addition, the Science and Technology Facilities Council (STFC) of the United Kingdom, the Max-Planck-Society (MPS), and the State of Niedersachsen/Germany supported the construction of Advanced Laser Interferometer Gravitational-Wave Observatory (aLIGO) and construction and operation of the GEO600 detector. Additional support for aLIGO was provided by the Australian Research Council. Virgo is funded, through the European Gravitational Observatory (EGO), by the French Centre National de Recherche Scientifique (CNRS), the Italian Istituto Nazionale di Fisica Nucleare (INFN) and the Dutch Nikhef, with contributions by institutions from Belgium, Germany, Greece, Hungary, Ireland, Japan, Monaco, Poland, Portugal, Spain.

This material is based upon work supported by NSF's LIGO Laboratory which is a major facility fully funded by the National Science Foundation. The authors are grateful for computational resources provided by the the LIGO Lab cluster at the LIGO Laboratory and supported by PHY-0757058 and PHY-0823459, the Pennsylvania State University's Institute for Computational and Data Sciences gravitational-wave cluster, and supported by OAC-2103662, PHY-2308881, PHY-2011865, OAC-2201445, OAC-2018299, and PHY-2207728. CJH and LT acknowledges support from the Nevada Center for Astrophysics, from NASA Grant No. 80NSSC23M0104. CJH also acknowledges support from the National Science Foundation through the Award No. PHY-2409727. CH Acknowledges generous support from the Eberly College of Science, the Department of Physics, the Institute for Gravitation and the Cosmos, the Institute for Computational and Data Sciences, and the Freed Early Career Professorship. M.W.C. acknowledges support from the National Science Foundation with grant numbers PHY-2308862 and PHY-2117997.

APPENDIX

A. DNS CATALOG

To construct the mass function for our ranking statistic, we compiled the most recent DNS catalog as of May 2025. Table 3 summarizes the total and component masses of these systems in the source frame. Compared with previous studies, our catalog adds nine systems relative to [Özel & Freire \(2016\)](#) and three relative to [Farrow et al. \(2019\)](#), excluding systems likely hosting a white-dwarf companion. Mass measurements for DNS observed in radio surveys are derived from Post-Keplerian (PK) parameters, which capture small relativistic effects in pulsar binaries ([Özel & Freire 2016](#)). The number of measurable PK parameters depends on the pulsar timing precision and determines whether individual component masses can be inferred. In our catalog, 13 systems have precise component-mass measurements, while six provide only the total mass, yielding a total of 19 events.

(a) Galactic DNS Systems with Precise Component Mass Measurement				
Pulsar Name	Total Mass (M_{\odot})	Pulsar Mass (M_{\odot})	Companion Mass (M_{\odot})	Reference
J0453+1559	2.734	1.559	1.174	Martinez et al. (2015)
J0737-3039	2.58708	1.3381	1.2489	Kramer et al. (2006)
B1534+12	2.678463	1.3330	1.3455	Fonseca et al. (2014)
J1756-2251	2.56999	1.341	1.230	Ferdman et al. (2014)
J1906+0746	2.6134	1.291	1.322	van Leeuwen et al. (2015)
B1913+16	2.828378	1.4398	1.3886	Weisberg et al. (2010)
B2127 + 11c	2.71279	1.358	1.354	Jacoby et al. (2006)
J1757-1854	2.73295	1.3384	1.3946	Cameron et al. (2018)
J0509+3801	2.81	1.34	1.46	Lynch et al. (2018)
J1913+1102	2.8887	1.62	1.27	Ferdman et al. (2020)
J1208-5936	2.586	1.26	1.32	Bernadich et al. (2023)
J1518+4904	2.7186	1.470	1.248	Tan et al. (2024)
J1828+2456	2.59	1.306	1.299	Haniewicz et al. (2020)
(b) Galactic DNS Systems without Precise Component Mass Measurement				
Pulsar Name	Total Mass (M_{\odot})	Pulsar Mass (M_{\odot})	Companion Mass (M_{\odot})	Reference
J1811-1736	2.57	< 1.64	> 0.93	Corongiu et al. (2007)
J1930-1852	2.59	< 1.32	> 1.30	Swiggum et al. (2015)
J1946+2052	2.50	< 1.31	> 1.18	Stovall et al. (2018)
J1901+0658	2.79	< 1.68	> 1.11	Su et al. (2024)
J1846-0513	2.6287	< 1.3455	> 1.2845	Zhao et al. (2024)
J1411+2251	2.538	< 1.62	> 0.92	Martinez et al. (2017)
(c) BNS Candidates of Gravitational Wave Events in GWTC Catalog				
Event Name	Total Mass (M_{\odot})	Primary Mass (M_{\odot})	Secondary Mass (M_{\odot})	Reference
GW170817 (low-spin prior)	2.74	1.36 - 1.60	1.17 - 1.36	Abbott et al. (2019)
GW170817 (high-spin prior)	2.82	1.36 - 2.26	0.86 - 1.36	Abbott et al. (2019)
GW190425 (low-spin prior)	3.3	1.60-1.87	1.46-1.69	Abbott et al. (2020)
GW190425 (high-spin prior)	3.4	1.61-2.52	1.12-1.68	Abbott et al. (2020)

Table 3. Galactic DNS catalog with measurement of multi-messenger event GW170817 by May 2025. All masses reported in the catalog are in source frame. There are total 19 systems discovered by radio surveys. (a) DNS catalog with precise component mass measurement. The subset contains 13 DNS systems. (b) DNS catalog without precise component mass measurement. The subset contains 6 DNS events, for which only the total mass is known due to insufficient determination of the PK parameters in these binary systems.

B. GWTC-4.0 RERANK AND TRIAL FACTORS

The GWTC-4 catalog reports GW231109_235456 (Abac et al. 2025a) as a sub-threshold candidate with a FAR of 631 per year in the GstLAL pipeline (Abac et al. 2025a). We re-ranked the GstLAL candidates from GWTC-4 using the DNS population model incorporated into the GstLAL stellar-mass template bank. Under this model, GW231109_235456 is identified as the highest-ranked trigger, with a FAR of 0.0084 per year and a false alarm probability (FAP) of 0.0045 (corresponding to $\sim 2.8\sigma$ under a Gaussian approximation). No additional candidates attained comparable significance in this re-ranking. Both the re-ranked results of the standard search and the targeted analysis consistently indicate that GW231109_235456 attains non-negligible significance under the DNS population prior.

In the GstLAL ranking statistic, detection significance is evaluated as the ratio of a signal-weighted likelihood to a noise-weighted likelihood. The mass model, representing the primary distinction between GWTC-4 and the re-rank, contributes only to the signal-weighted term. The noise background can thus be considered effectively unchanged, and the observed reduction in FAR can be attributed predominantly to the difference in signal volume from the prior. To account for the FAR shift, of order $\sim 10^{-5}$, we estimate the ratio of the corresponding prior volumes, yielding:

$$\left(\frac{\int_{\text{DNS}} P(t_k, \rho | H_{\text{Power-Law}}) H_D^3(t_k) dV_{t_k}}{\int_{\text{stellar-mass-bank}} P(t_k, \rho | H_{\text{Power-Law}}) H_D^3(t_k) dV_{t_k}} \right) \bigg/ \left(\frac{\int_{\text{DNS}} P(t_k, \rho | H_{\text{DNS}}) H_D^3(t_k) dV_{t_k}}{\int_{\text{stellar-mass-bank}} P(t_k, \rho | H_{\text{DNS}}) H_D^3(t_k) dV_{t_k}} \right) \quad (\text{B1})$$

The first term (left) represents the volume of DNS masses within the Power-Law mass model, integrated over the DNS mass range, $[1.1, 2.1] M_\odot$, as specified in Sec 2.2. Here, $P(t_k, \rho | H_{\text{Power-Law}})$ denotes the mass weighting of the Power-Law model for each template t_k at SNR ρ , H_D is the horizon distance of template t_k , and dV_{t_k} is the corresponding volume element. The denominator, obtained by integrating the weighting over the full template bank parameter space, serves as a normalization factor representing the total prior volume across the search range. The second term (right) represents the volume of DNS masses within the DNS mass model, normalized by the volume of the full bank. This yields a value close to unity, as the DNS mass model predominantly encompasses DNS candidates while excluding other signals. It does not reach exactly one, however, because certain high-mass templates still occupy a nonzero weighting in the stellar mass bank. The prior volume ratio is approximately 5×10^{-7} , roughly consistent with the FAR ratio between the GWTC-4.0 and rerank analyses for this trigger. The enhanced sensitivity that enables the detection of this event likely comes at the expense of reduced sensitivity in the higher-mass region of GWTC-4.

C. DNS BANK PERFORMANCE

We test the recoverability of the DNS-targeted bank against the DNS population and compare its performance with that of the stellar-mass bank in the same parameter region. To do so, we evaluate the bank using the sampled DNS population described in Sec 2.1. The calculation of mismatch is performed with SBANK software (Ajith et al. 2014; Capano et al. 2016; Harry et al. 2009; Privitera et al. 2014) where the mismatch is defined as $1 - \text{fitting factor (FF)}$ (Privitera et al. 2014; Apostolatos 1995):

$$FF(\hat{u}_s, u) = \max_k \langle \hat{u}_k | \hat{u}_s \rangle \quad (\text{C2})$$

between the bank waveforms and the simulated signals. Details of the bank simulation methodology can be found in Sakon et al. (2024); Hanna et al. (2025). Fig 4(a) shows the mismatch distribution of the DNS bank compared to the stellar-mass bank for the DNS population. Fig 4(b) illustrates the effectiveness of the DNS bank across the (m1, m2) parameter space. Overall, we find that the designated bank yields an expected sensitivity-volume improvement of about 2-4 %. If including the horizon factor due to filtering without the duration cut, we can get around 4-8 % sensitivity improvement.

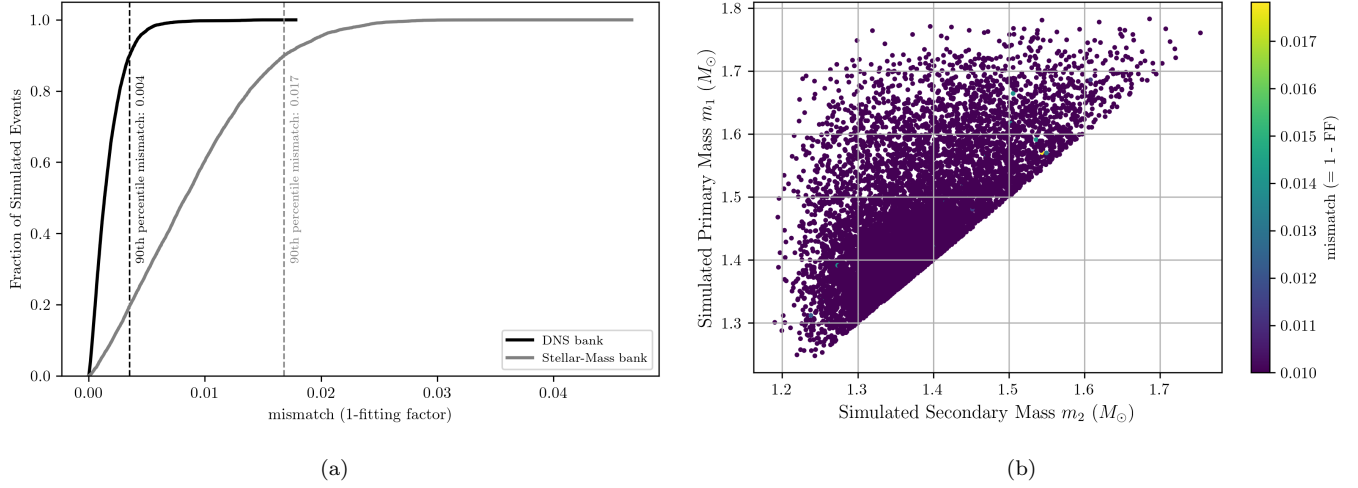


Figure 4. Cumulative density function plot of mismatch. (a) For the designated DNS bank, the 90th percentile mismatch between templates and simulations is below 0.004, compared to 0.017 for the all-sky bank. This corresponds empirically to an expected 2% improvement in sensitivity volume. (b) Mismatch distribution of the DNS bank across the (m_1, m_2) parameter space. The non-uniform density reflects the two-component Gaussian sampling of the simulated population.

REFERENCES

- 2025, arXiv e-prints. <https://arxiv.org/abs/2508.18083>
- Aasi, J., et al. 2015, *Class. Quant. Grav.*, 32, 074001, doi: [10.1088/0264-9381/32/7/074001](https://doi.org/10.1088/0264-9381/32/7/074001)
- Abac, A. G., et al. 2025a. <https://arxiv.org/abs/2508.18082>
- . 2025b, arXiv e-prints. <https://arxiv.org/abs/2508.18081>
- . 2025c, arXiv e-prints. <https://arxiv.org/abs/2508.18080>
- Abbott, B. P., et al. 2016, *Living Rev. Rel.*, 19, 1, doi: [10.1007/s41114-020-00026-9](https://doi.org/10.1007/s41114-020-00026-9)
- . 2017a, *Phys. Rev. Lett.*, 119, 161101, doi: [10.1103/PhysRevLett.119.161101](https://doi.org/10.1103/PhysRevLett.119.161101)
- . 2017b, *Astrophys. J. Lett.*, 848, L12, doi: [10.3847/2041-8213/aa91c9](https://doi.org/10.3847/2041-8213/aa91c9)
- . 2019, *Phys. Rev. X*, 9, 011001, doi: [10.1103/PhysRevX.9.011001](https://doi.org/10.1103/PhysRevX.9.011001)
- . 2020, *Astrophys. J. Lett.*, 892, L3, doi: [10.3847/2041-8213/ab75f5](https://doi.org/10.3847/2041-8213/ab75f5)
- Abbott, R., et al. 2023, *Phys. Rev. X*, 13, 011048, doi: [10.1103/PhysRevX.13.011048](https://doi.org/10.1103/PhysRevX.13.011048)
- Acernese, F., et al. 2015, *Class. Quant. Grav.*, 32, 024001, doi: [10.1088/0264-9381/32/2/024001](https://doi.org/10.1088/0264-9381/32/2/024001)
- Ade, P. A. R., et al. 2016, *Astron. Astrophys.*, 594, A13, doi: [10.1051/0004-6361/201525830](https://doi.org/10.1051/0004-6361/201525830)
- Ajith, P., Fotopoulos, N., Privitera, S., et al. 2014, *Physical Review D*, 89, 084041, doi: [10.1103/physrevd.89.084041](https://doi.org/10.1103/physrevd.89.084041)
- Alsing, J., Silva, H. O., & Berti, E. 2018, *Mon. Not. Roy. Astron. Soc.*, 478, 1377, doi: [10.1093/mnras/sty1065](https://doi.org/10.1093/mnras/sty1065)
- Apostolatos, T. A. 1995, *Phys. Rev. D*, 52, 605, doi: [10.1103/PhysRevD.52.605](https://doi.org/10.1103/PhysRevD.52.605)
- Ashton, G., et al. 2019, *Astrophys. J. Suppl.*, 241, 27, doi: [10.3847/1538-4365/ab06fc](https://doi.org/10.3847/1538-4365/ab06fc)
- Bernadich, I. M. C., et al. 2023, *Astron. Astrophys.*, 678, A187, doi: [10.1051/0004-6361/202346953](https://doi.org/10.1051/0004-6361/202346953)
- Buikema, A., et al. 2020, *Phys. Rev. D*, 102, 062003, doi: [10.1103/PhysRevD.102.062003](https://doi.org/10.1103/PhysRevD.102.062003)
- Cameron, A. D., et al. 2018, *Mon. Not. Roy. Astron. Soc.*, 475, L57, doi: [10.1093/mnrasl/sly003](https://doi.org/10.1093/mnrasl/sly003)
- Cannon, K., Hanna, C., & Keppel, D. 2012, *Phys. Rev. D*, 85, 081504, doi: [10.1103/PhysRevD.85.081504](https://doi.org/10.1103/PhysRevD.85.081504)
- . 2013, *Phys. Rev. D*, 88, 024025, doi: [10.1103/PhysRevD.88.024025](https://doi.org/10.1103/PhysRevD.88.024025)
- Cannon, K., et al. 2020. <https://arxiv.org/abs/2010.05082>
- Capano, C., Harry, I., Privitera, S., & Buonanno, A. 2016, *Physical Review D*, 93, 124007, doi: [10.1103/physrevd.93.124007](https://doi.org/10.1103/physrevd.93.124007)
- Capote, E., et al. 2025, *Phys. Rev. D*, 111, 062002, doi: [10.1103/PhysRevD.111.062002](https://doi.org/10.1103/PhysRevD.111.062002)
- Chatziioannou, K., Haster, C.-J., & Zimmerman, A. 2018, *Phys. Rev. D*, 97, 104036, doi: [10.1103/PhysRevD.97.104036](https://doi.org/10.1103/PhysRevD.97.104036)
- Clesse, S., & Garcia-Bellido, J. 2022, *Phys. Dark Univ.*, 38, 101111, doi: [10.1016/j.dark.2022.101111](https://doi.org/10.1016/j.dark.2022.101111)
- Colleoni, M., Ramis Vidal, F. A., Johnson-McDaniel, N. K., et al. 2025, *Phys. Rev. D*, 111, 064025, doi: [10.1103/PhysRevD.111.064025](https://doi.org/10.1103/PhysRevD.111.064025)
- Corongiu, A., Kramer, M., Stappers, B. W., et al. 2007, *Astron. Astrophys.*, 462, 703, doi: [10.1051/0004-6361:20054385](https://doi.org/10.1051/0004-6361:20054385)
- Coulter, D. A., et al. 2025, *Astrophys. J.*, 988, 169, doi: [10.3847/1538-4357/ade0b3](https://doi.org/10.3847/1538-4357/ade0b3)
- Dietrich, T., Samajdar, A., Khan, S., et al. 2019, *Phys. Rev. D*, 100, 044003, doi: [10.1103/PhysRevD.100.044003](https://doi.org/10.1103/PhysRevD.100.044003)
- Drout, M. R., et al. 2017, *Science*, 358, 1570, doi: [10.1126/science.aag0049](https://doi.org/10.1126/science.aag0049)
- Essick, R. 2025, monte-carlo-vt, <https://git.ligo.org/reed.essick/monte-carlo-vt>
- Essick, R., & et al. 2025, gw-distributions, <https://git.ligo.org/reed.essick/gw-distributions>
- Essick, R., et al. 2025. <https://arxiv.org/abs/2508.10638>
- Evans, P. A., et al. 2017, *Science*, 358, 1565, doi: [10.1126/science.aap9580](https://doi.org/10.1126/science.aap9580)
- Ewing, B., et al. 2024, *Phys. Rev. D*, 109, 042008, doi: [10.1103/PhysRevD.109.042008](https://doi.org/10.1103/PhysRevD.109.042008)
- Farrow, N., Zhu, X.-J., & Thrane, E. 2019, *Astrophys. J.*, 876, 18, doi: [10.3847/1538-4357/ab12e3](https://doi.org/10.3847/1538-4357/ab12e3)
- Ferdman, R. D., et al. 2014, *Mon. Not. Roy. Astron. Soc.*, 443, 2183, doi: [10.1093/mnras/stu1223](https://doi.org/10.1093/mnras/stu1223)
- . 2020, *Nature*, 583, 211, doi: [10.1038/s41586-020-2439-x](https://doi.org/10.1038/s41586-020-2439-x)
- Foley, R. J., Coulter, D. A., Kilpatrick, C. D., et al. 2020, *Mon. Not. Roy. Astron. Soc.*, 494, 190, doi: [10.1093/mnras/staa725](https://doi.org/10.1093/mnras/staa725)
- Fong, H. K. Y. 2018, Phd thesis, University of Toronto
- Fonseca, E., Stairs, I. H., & Thorsett, S. E. 2014, *Astrophys. J.*, 787, 82, doi: [10.1088/0004-637X/787/1/82](https://doi.org/10.1088/0004-637X/787/1/82)
- Galaudage, S., Adamcewicz, C., Zhu, X.-J., Stevenson, S., & Thrane, E. 2021, *Astrophys. J. Lett.*, 909, L19, doi: [10.3847/2041-8213/abe7f6](https://doi.org/10.3847/2041-8213/abe7f6)
- Ganapathy, D., et al. 2023, *Phys. Rev. X*, 13, 041021, doi: [10.1103/PhysRevX.13.041021](https://doi.org/10.1103/PhysRevX.13.041021)
- Gupta, A., Gerosa, D., Arun, K. G., et al. 2020, *Phys. Rev. D*, 101, 103036, doi: [10.1103/PhysRevD.101.103036](https://doi.org/10.1103/PhysRevD.101.103036)
- Gupta, T., & Cornish, N. J. 2024, *Phys. Rev. D*, 109, 064040, doi: [10.1103/PhysRevD.109.064040](https://doi.org/10.1103/PhysRevD.109.064040)
- Haniewicz, H. T., Ferdman, R. D., Freire, P. C. C., et al. 2020, *Mon. Not. Roy. Astron. Soc.*, 500, 4620, doi: [10.1093/mnras/staa3466](https://doi.org/10.1093/mnras/staa3466)

- Hanna, C. 2024, manifold, <https://git.ligo.org/chad-hanna/manifold>, GitHub
- Hanna, C., et al. 2020, *Phys. Rev. D*, 101, 022003, doi: [10.1103/PhysRevD.101.022003](https://doi.org/10.1103/PhysRevD.101.022003)
- . 2023, *Phys. Rev. D*, 108, 042003, doi: [10.1103/PhysRevD.108.042003](https://doi.org/10.1103/PhysRevD.108.042003)
- . 2025, *Phys. Rev. D*, 112, 044013, doi: [10.1103/c97v-bmj8](https://doi.org/10.1103/c97v-bmj8)
- Hannam, M., Schmidt, P., Bohé, A., et al. 2014, *Phys. Rev. Lett.*, 113, 151101, doi: [10.1103/PhysRevLett.113.151101](https://doi.org/10.1103/PhysRevLett.113.151101)
- Harry, I. W., Allen, B., & Sathyaprakash, B. S. 2009, *Physical Review D*, 80, 104014, doi: [10.1103/physrevd.80.104014](https://doi.org/10.1103/physrevd.80.104014)
- Hulse, R. A., & Taylor, J. H. 1975, *Astrophys. J. Lett.*, 195, L51, doi: [10.1086/181708](https://doi.org/10.1086/181708)
- Husa, S., Khan, S., Hannam, M., et al. 2016, *Physical Review D*, 93, 044006, doi: [10.1103/physrevd.93.044006](https://doi.org/10.1103/physrevd.93.044006)
- Jacoby, B. A., Cameron, P. B., Jenet, F. A., et al. 2006, *Astrophys. J. Lett.*, 644, L113, doi: [10.1086/505742](https://doi.org/10.1086/505742)
- Jia, W., et al. 2024, *Science*, 385, 1318, doi: [10.1126/science.ado8069](https://doi.org/10.1126/science.ado8069)
- Joshi, P., et al. 2025a. <https://arxiv.org/abs/2506.06497>
- . 2025b. <https://arxiv.org/abs/2505.23959>
- Khan, S., Husa, S., Hannam, M., et al. 2016a, *Physical Review D*, 93, 044007, doi: [10.1103/physrevd.93.044007](https://doi.org/10.1103/physrevd.93.044007)
- . 2016b, *Phys. Rev. D*, 93, 044007, doi: [10.1103/PhysRevD.93.044007](https://doi.org/10.1103/PhysRevD.93.044007)
- Kilpatrick, C. D., et al. 2017, *Science*, 358, 1583, doi: [10.1126/science.aaq0073](https://doi.org/10.1126/science.aaq0073)
- Kiziltan, B., Kottas, A., & Thorsett, S. E. 2013, *The Astrophysical Journal*, 778, doi: [10.1088/0004-637X/778/1/66](https://doi.org/10.1088/0004-637X/778/1/66)
- Kramer, M., et al. 2006, *Science*, 314, 97, doi: [10.1126/science.1132305](https://doi.org/10.1126/science.1132305)
- Kyutoku, K., Fujibayashi, S., Hayashi, K., et al. 2020, *Astrophys. J. Lett.*, 890, L4, doi: [10.3847/2041-8213/ab6e70](https://doi.org/10.3847/2041-8213/ab6e70)
- Landry, P., & Read, J. S. 2021, *Astrophys. J. Lett.*, 921, L25, doi: [10.3847/2041-8213/ac2f3e](https://doi.org/10.3847/2041-8213/ac2f3e)
- Littenberg, T. B., & Cornish, N. J. 2015, *Phys. Rev. D*, 91, 084034, doi: [10.1103/PhysRevD.91.084034](https://doi.org/10.1103/PhysRevD.91.084034)
- LVK. 2018, GraceDB: The Gravitational-Wave Candidate Event Database, Tech. Rep. LIGO-T1400365-v5, LIGO Project. <https://dcc.ligo.org/LIGO-T1400365/public>
- Lynch, R. S., et al. 2018, *Astrophys. J.*, 859, 93, doi: [10.3847/1538-4357/aabf8a](https://doi.org/10.3847/1538-4357/aabf8a)
- Magee, R., et al. 2019, *Astrophys. J. Lett.*, 878, L17, doi: [10.3847/2041-8213/ab20cf](https://doi.org/10.3847/2041-8213/ab20cf)
- Martinez, J. G., Stovall, K., Freire, P. C. C., et al. 2015, *Astrophys. J.*, 812, 143, doi: [10.1088/0004-637X/812/2/143](https://doi.org/10.1088/0004-637X/812/2/143)
- . 2017, *Astrophys. J. Lett.*, 851, L29, doi: [10.3847/2041-8213/aa9d87](https://doi.org/10.3847/2041-8213/aa9d87)
- McCully, C., et al. 2017, *Astrophys. J. Lett.*, 848, L32, doi: [10.3847/2041-8213/aa9111](https://doi.org/10.3847/2041-8213/aa9111)
- Messick, C., et al. 2017, *Phys. Rev. D*, 95, 042001, doi: [10.1103/PhysRevD.95.042001](https://doi.org/10.1103/PhysRevD.95.042001)
- Morisaki, S., Smith, R., Tsukada, L., et al. 2023, *Phys. Rev. D*, 108, 123040, doi: [10.1103/PhysRevD.108.123040](https://doi.org/10.1103/PhysRevD.108.123040)
- Nelemans, G. 2003, *AIP Conf. Proc.*, 686, 263, doi: [10.1063/1.1629441](https://doi.org/10.1063/1.1629441)
- Owen, B. J. 1996, *Phys. Rev. D*, 53, 6749, doi: [10.1103/PhysRevD.53.6749](https://doi.org/10.1103/PhysRevD.53.6749)
- Özel, F., & Freire, P. 2016, *Ann. Rev. Astron. Astrophys.*, 54, 401, doi: [10.1146/annurev-astro-081915-023322](https://doi.org/10.1146/annurev-astro-081915-023322)
- Ozel, F., Psaltis, D., Narayan, R., & Villarreal, A. S. 2012, *Astrophys. J.*, 757, 55, doi: [10.1088/0004-637X/757/1/55](https://doi.org/10.1088/0004-637X/757/1/55)
- Paek, G. S. H., et al. 2024, *Astrophys. J.*, 960, 113, doi: [10.3847/1538-4357/ad0238](https://doi.org/10.3847/1538-4357/ad0238)
- Pian, E., et al. 2017, *Nature*, 551, 67, doi: [10.1038/nature24298](https://doi.org/10.1038/nature24298)
- Price-Whelan, A. M., et al. 2022, *Astrophys. J.*, 935, 167, doi: [10.3847/1538-4357/ac7c74](https://doi.org/10.3847/1538-4357/ac7c74)
- Privitera, S., Mohapatra, S. R. P., Ajith, P., et al. 2014, *Phys. Rev. D*, 89, 024003, doi: [10.1103/PhysRevD.89.024003](https://doi.org/10.1103/PhysRevD.89.024003)
- Ray, A., et al. 2023. <https://arxiv.org/abs/2306.07190>
- Romero-Shaw, I. M., Farrow, N., Stevenson, S., Thrane, E., & Zhu, X.-J. 2020a, *Mon. Not. Roy. Astron. Soc.*, 496, L64, doi: [10.1093/mnras/slaa084](https://doi.org/10.1093/mnras/slaa084)
- Romero-Shaw, I. M., et al. 2020b, *Mon. Not. Roy. Astron. Soc.*, 499, 3295, doi: [10.1093/mnras/staa2850](https://doi.org/10.1093/mnras/staa2850)
- Sachdev, S., et al. 2019. <https://arxiv.org/abs/1901.08580>
- Safarzadeh, M., Ramirez-Ruiz, E., & Berger, E. 2020, *Astrophys. J.*, 900, 13, doi: [10.3847/1538-4357/aba596](https://doi.org/10.3847/1538-4357/aba596)
- Sakon, S., et al. 2024, *Phys. Rev. D*, 109, 044066, doi: [10.1103/PhysRevD.109.044066](https://doi.org/10.1103/PhysRevD.109.044066)
- Singh, D., Ryan, M., Magee, R., et al. 2021, *Physical Review D*, 104, 044015
- Smartt, S. J., et al. 2017, *Nature*, 551, 75, doi: [10.1038/nature24303](https://doi.org/10.1038/nature24303)
- Smith, R., Field, S. E., Blackburn, K., et al. 2016, *Phys. Rev. D*, 94, 044031, doi: [10.1103/PhysRevD.94.044031](https://doi.org/10.1103/PhysRevD.94.044031)
- Soni, S., et al. 2025, *Class. Quant. Grav.*, 42, 085016, doi: [10.1088/1361-6382/adc4b6](https://doi.org/10.1088/1361-6382/adc4b6)
- Stovall, K., et al. 2018, *Astrophys. J. Lett.*, 854, L22, doi: [10.3847/2041-8213/aaad06](https://doi.org/10.3847/2041-8213/aaad06)

- Su, W. Q., et al. 2024, *Mon. Not. Roy. Astron. Soc.*, 530, 1506, doi: [10.1093/mnras/stae888](https://doi.org/10.1093/mnras/stae888)
- Swiggum, J. K., et al. 2015, *Astrophys. J.*, 805, 156, doi: [10.1088/0004-637X/805/2/156](https://doi.org/10.1088/0004-637X/805/2/156)
- Tan, C. M., Fonseca, E., Crowter, K., et al. 2024, *Astrophys. J.*, 966, 26, doi: [10.3847/1538-4357/ad28b2](https://doi.org/10.3847/1538-4357/ad28b2)
- Thorsett, S. E., & Chakrabarty, D. 1999, *Astrophys. J.*, 512, 288, doi: [10.1086/306742](https://doi.org/10.1086/306742)
- Tse, M., et al. 2019, *Phys. Rev. Lett.*, 123, 231107, doi: [10.1103/PhysRevLett.123.231107](https://doi.org/10.1103/PhysRevLett.123.231107)
- Tsukada, L., et al. 2023, *Phys. Rev. D*, 108, 043004, doi: [10.1103/PhysRevD.108.043004](https://doi.org/10.1103/PhysRevD.108.043004)
- Valenti, S., Sand, D. J., Yang, S., et al. 2017, *Astrophys. J. Lett.*, 848, L24, doi: [10.3847/2041-8213/aa8edf](https://doi.org/10.3847/2041-8213/aa8edf)
- van Leeuwen, J., et al. 2015, *Astrophys. J.*, 798, 118, doi: [10.1088/0004-637X/798/2/118](https://doi.org/10.1088/0004-637X/798/2/118)
- Weisberg, J. M., Nice, D. J., & Taylor, J. H. 2010, *Astrophys. J.*, 722, 1030, doi: [10.1088/0004-637X/722/2/1030](https://doi.org/10.1088/0004-637X/722/2/1030)
- Yagi, K., & Yunes, N. 2016, *Class. Quant. Grav.*, 33, 13LT01, doi: [10.1088/0264-9381/33/13/13LT01](https://doi.org/10.1088/0264-9381/33/13/13LT01)
- Ye, C., & Fishbach, M. 2021, *Phys. Rev. D*, 104, 043507, doi: [10.1103/PhysRevD.104.043507](https://doi.org/10.1103/PhysRevD.104.043507)
- Zhang, J., Yang, Y., Zhang, C., et al. 2019, *Mon. Not. Roy. Astron. Soc.*, 488, 5020, doi: [10.1093/mnras/stz2020](https://doi.org/10.1093/mnras/stz2020)
- Zhao, D., et al. 2024, *Astrophys. J. Lett.*, 964, L7, doi: [10.3847/2041-8213/ad2fb3](https://doi.org/10.3847/2041-8213/ad2fb3)
- Zhu, X., Thrane, E., Osłowski, S., Levin, Y., & Lasky, P. D. 2018, *Phys. Rev. D*, 98, 043002, doi: [10.1103/PhysRevD.98.043002](https://doi.org/10.1103/PhysRevD.98.043002)